Acta Materialia 120 (2016) 216–227

Contents lists available at ScienceDirect

Acta Materialia

journal homepage: www.elsevier.com/locate/actamat

Full length article

Effects of welding and post-weld heat treatments on nanoscale precipitation and mechanical properties of an ultra-high strength steel hardened by NiAl and Cu nanoparticles

Z.B. Jiao [a], J.H. Luan [a], W. Guo [b], J.D. Poplawsky [b], C.T. Liu [a, *]

[a] Center for Advanced Structural Materials, Department of Mechanical and Biomedical Engineering, College of Science and Engineering, City University of Hong Kong, Hong Kong, China
[b] Center for Nanophase Materials Sciences, Oak Ridge National Laboratory, Oak Ridge, TN 37831, USA

ARTICLE INFO

Article history:
Received 5 August 2016
Received in revised form
22 August 2016
Accepted 24 August 2016
Available online 1 September 2016

Keywords:
Welding
Ultra-high strength steel
Precipitation
Mechanical property
Structure-property relationship

ABSTRACT

The effects of welding and post-weld heat treatment (PWHT) on nanoscale co-precipitation, grain structure, and mechanical properties of an ultra-high strength steel were studied through a combination of atom probe tomography (APT) and mechanical tests. Our results indicate that the welding process dissolves all pre-existing nanoparticles and causes grain coarsening in the fusion zone, resulting in a soft and ductile weld without any cracks in the as-welded condition. A 550 °C PWHT induces fine-scale re-precipitation of NiAl and Cu co-precipitates with high number densities and ultra-fine sizes, leading to a large recovery of strength but a loss of ductility with intergranular failure, whereas a 600 °C PWHT gives rise to coarse-scale re-precipitation of nanoparticles together with the formation of a small amount of reverted austenite, resulting in a great recovery in both strength and ductility. Our analysis indicates that the degree of strength recovery is dependent mainly upon the re-precipitation microstructure of nanoparticles, together with grain size and reversion of austenite, while the ductility recovery is sensitive to the grain-boundary structure. APT reveals that the grain-boundary segregation of Mn and P may be the main reason for the 550 °C embrittlement, and the enhanced ductility at 600 °C is ascribed to a possible reduction of the segregation and reversion of austenite.

1. Introduction

Ultra-high strength steels have received a growing interest in recent years due to their high potential for weight reduction and performance improvement for various lightweight applications, such as aerospace, vehicles, shipbuilding, and wind energy. In the fabrication of these structures, welding is one of the most important and versatile processes available to industry for joining steels, and a good weldability is a highly desirable feature of ultra-high strength steels. From a metallurgical point of view, although carbon is one of the most potent strengthening elements in steels, too much carbon is extremely harmful to weldability, through increasing the probabilities of forming brittle martensite and hence the risk of cold-cracking after welding [1]. As such, ferrous metallurgy emphases have been increasingly placed on the development of ultra-high strength steels with reduced carbon contents for improving weldability. Nanoparticles strengthened ferritic/martensitic steels represent an important class of advanced steels which, by virtue of appropriate composition and thermo-mechanical processing, exhibit both high strength and good ductility while minimizing the use of carbon and other alloying additions [2–8]. In particular, the precipitation of coherent nanoparticles, such as body-centered cubic (bcc) Cu-rich nanoclusters [2–5,9–12] and B2-ordered NiAl intermetallic nanoparticles [13–17], is very appealing, because they can precipitate on a sufficiently fine scale (less than 5 nm in diameter), providing an extremely high strengthening response. Currently, research is starting to emerge on the weldability of this class of high-strength steels, mostly of Cu-rich nanoclusters strengthened steels [18–23]. Previous welding studies showed that the hardness of heat-affected zone (HAZ) and fusion zone (FZ) of Cu-strengthened steels was under-matched to the base metal (BM), which was considered to be due to the partial dissolution of pre-existing Cu-rich nanoclusters within the HAZ and full dissolution of

* Corresponding author.
E-mail address: chainliu@cityu.edu.hk (C.T. Liu).

http://dx.doi.org/10.1016/j.actamat.2016.08.066
1359-6454/

nanoclusters within the FZ, as characterized by atom probe tomography (APT) [18–21]. It has been found that the re-precipitation of nanoparticles can be achieved by designing an appropriate post-weld heat treatment (PWHT) or multi-pass welding procedure, which provides a promising way to recover the mechanical properties of welds [22,23].

Recent studies reveal that the co-precipitation of multiple types of nanoparticles is more attractive, as compared with precipitation of a dispersion of a single type of nanoparticles, since the co-precipitation approach may lead to a superior combination of different properties resulting from the synergistic combination of multiple types of nanoparticles with different compositions, microstructures, and micromechanical properties [24–30]. For example, through the optimization of alloy compositions, the co-precipitation of Cu-rich and NiAl-based nanoparticles can be achieved, which offers a promising way to effectively strengthen steels to as high as 2000 MPa while maintaining a good ductility of approximately 10% elongation [28,29]. To date, however, the welding properties of this new class of nanoscale co-precipitation strengthened steels is poorly understood, and their post-weld microstructure-property relationship remains unclear. For an understanding of and eventually control over the microstructure and mechanical property response to welding, it is of fundamental importance to understand the effect of welding and PWHT on the nanoscale co-precipitation, grain structures, and mechanical properties of this new class of nanoscale co-precipitation strengthened steels with ultra-high strength.

The purpose of this study is to elucidate the mechanism of the precipitate microstructure and grain structure evolution during welding and PWHT, and further to correlate the microstructure with bulk mechanical properties of a NiAl/Cu co-precipitation strengthened steel. The precipitates characteristics, including the size, number density, composition, and solute partitioning behavior of NiAl and Cu co-precipitates were thoroughly investigated by APT. Particular attention was paid to understanding the basic mechanism involved in the precipitate dissolution and re-precipitation and to further elucidate the key factors governing the weld strength and ductility.

2. Experimental

The material investigated in this study is a high-strength steel with a composition of Fe–5Ni–2Al–3Mn–1.5Cu–1.5Mo–1.5W–0.07Nb–0.05C–0.01B (wt%) [29]. Alloy ingots were prepared by arc-melting a mixture of the constituent elements with purity better than 99.9 wt% in a Ti-gettered high-purity argon atmosphere. Repeated melting was carried out at least five times to ensure the chemical homogeneity. The melted alloys were then drop-cast into a copper mold with dimensions of $15 \times 30 \times 100$ mm^3. The resulting plates were cold rolled by multiple passes with a total reduction of ~66% and then solution-treated for 30 min at 900 °C, followed by water quenching, and then aged isothermally at 550 °C for 2 h, resulting in the formation of ~3-nm NiAl and Cu co-precipitates [29].

4-mm-thick plates were welded using the gas tungsten arc welding (GTAW) technique, in which an arc was established between a non-consumable tungsten electrode and the work piece in an ultra-high purity argon atmosphere. The welding was performed with a welding power of ~2 kW and a travel speed of ~3 mm/s. The as-welded plates (which will be called hereafter the AW state) were post-weld heat treated at 550 °C and 600 °C for 30 min, which will be referred to as PWHT-550 and PWHT-600, respectively.

Transverse cross-sections of the AW, PWHT-550, and PWHT-600 samples perpendicular to the welding direction were polished to a final surface finish of 0.05 μm using standard mechanical polishing procedures. Hardness measurements were conducted on the polished surface of the samples using a Vickers hardness tester with a load of 2 N for 15 s. Tensile samples with a cross-section of 3.2×1 mm^2 and a gauge length of 15 mm were cut by electro-discharge machining, and ground careful on each side with SiC paper through 4000 grit. Tensile tests along the rolling direction of the samples were conducted on an MTS tensile testing machine at a strain rate of 10^{-3} s^{-1}. Two specimens were tested for each condition, and the average values were reported. Fracture surfaces were examined by scanning electron microscopy (SEM).

Needle-shaped specimens required for APT were fabricated by lift-outs and annular milled in a FEI Nova 200 focused ion beam/scanning electron microscope (FIB/SEM) [31,32]. The APT characterizations were performed in a local electrode atom probe (CAMEACA LEAP 4000X HR). The specimens were analyzed at 50 K in voltage mode, a pulse repetition rate of 200 kHz, a pulse fraction of 20%, and an evaporation detection rate of 0.5% atom per pulse. Imago Visualization and Analysis Software (IVAS) version 3.6.12 was used for creating the 3D reconstructions and data analysis. The equivalent spherical particle radius, R, was determined by Ref. [33]:

$$R = \left(\frac{3V_p}{4\pi}\right)^{\frac{1}{3}}, \tag{1}$$

V_p is the volume of the particle as defined by the volume within the interface defined using IVAS 3.6.12. The particle number density, N, were calculated from Ref. [33]:

$$N = \frac{N_p}{V}, \tag{2}$$

where N_p is the number of fully-contained plus 50% of the partially-contained particles within the volume, and V is the total volume of the APT reconstruction.

3. Results

3.1. Mechanical properties

The average hardness profiles measured along the transverse cross section of the welds in the AW, PWHT-550, and PWHT-600

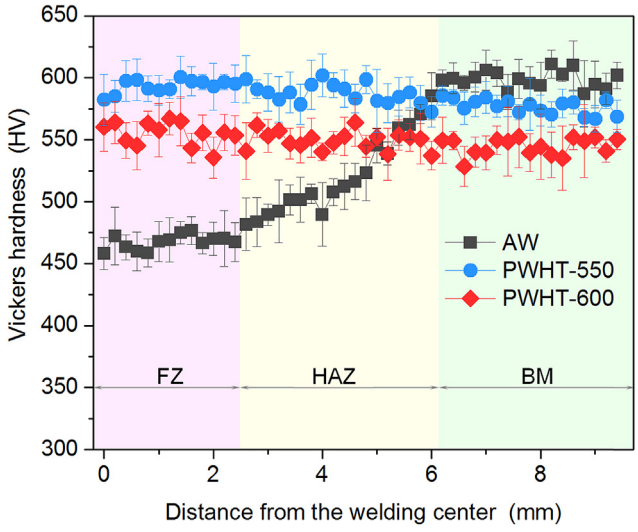

Fig. 1. Hardness profiles across the fusion zone, heat-affected zone and base metal in the as-welded and post-weld heat treated conditions.